Biophysical Reviews manuscript No.
(will be inserted by the editor)

Entropic stabilization of the folded states of RNA due to macromolecular crowding

Natalia A. Denesyuk · D. Thirumalai

We dedicate this article to Allen P. Minton, who has been a pioneer in recognizing the importance of crowding effects in biology and established methods to quantify them through theory and experiments.

Received: date / Accepted: date

Abstract We review the effects of macromolecular crowding on the folding of RNA by considering the simplest scenario when excluded volume interactions between crowding particles and RNA dominate. Using human telomerase enzyme as an example, we discuss how crowding can alter the equilibrium between pseudoknot and hairpin states of the same RNA molecule — a key aspect of crowder-RNA interactions. We summarize data showing that the crowding effect is significant

Natalia A. Denesyuk

Biophysics Program, Institute for Physical Science and Technology, University of Maryland, College Park, Maryland 20742

D. Thirumalai

Biophysics Program, Institute for Physical Science and Technology and Department of Chemistry and Biochemistry, University of Maryland, College Park, Maryland 20742

Tel.: +1-301-405-4803

Fax: +1-301-314-9404

E-mail: thirum@umd.edu

only if the size of the spherical crowding particle is smaller than the radius of gyration of the RNA in the absence of crowding particles. The implication for function of the wild type and mutants of human telomerase is outlined by using a relationship between enzyme activity and its conformational equilibrium. In addition, we discuss the interplay between macromolecular crowding and ionic strength of the RNA buffer. Finally, we briefly review recent experiments which illustrate the connection between excluded volume due to macromolecular crowding and the thermodynamics of RNA folding.

Keywords Crowding · Excluded volume · RNA · Telomerase · Enzyme activity

1 Introduction

The cytosol is crowded and replete with macromolecules such as ribosomes, lipids, proteins, and RNA. Estimates show that the volume fraction (ϕ) of these macromolecules, collectively referred to as crowding agents, can exceed 0.2. Spontaneous folding of nascent proteins and RNA in the crowded environment can be different from *in vitro* experiments that are typically conducted under infinite dilution. Minton, who has made pioneering contributions in elucidating the importance of crowding in biophysics, was the first to recognize that the thermodynamics of folding, association, and biochemical reactions can be altered by crowding agents (Minton, 1981, 2001, 2005; Hall and Minton, 2003; Zhou et al, 2008). More recently there has been much interest in the study of crowding effects on folding and function of proteins (Cheung et al, 2005; Homouz et al, 2008; Dhar et al, 2010; Elcock, 2010), which was inspired by the insightful studies initiated by Minton.

Describing even the simplest process, namely, the transition between folded and unfolded states of proteins and RNA under crowded conditions is complicated because the nature of the effective interactions between the crowding agents and the polypeptide or polynucleotide chains is not fully understood. However, to a first approximation, the dominant effect of crowding agents is to exclude the molecule of interest from the volume occupied by crowders. If excluded volume interactions dominate (an assumption that has to be tested before the theory can be applied to analyze experiments), then the stability of the folded state of the protein or RNA is enhanced, compared to the case when $\phi = 0$. In this case, the loss in entropy of the folded state due to crowding is much less than that of the unfolded state, resulting in the stabilization of the folded state. The entropic stabilization of the

folded state (Cheung et al, 2005; Minton, 2005) in the presence of crowding agents has been firmly established theoretically in a number of studies.

Most of the studies on the effects of crowding on self-assembly process have been on the folding of proteins. Recently, it has been recognized that crowding agents could have a significant impact on the folding of RNA (Pincus et al, 2008; Kilburn et al, 2010; Denesyuk and Thirumalai, 2011). Simple theoretical arguments and coarse-grained simulations were used to show that crowding can modestly stabilize RNA secondary structures (Pincus et al, 2008). However, RNA requires counterions (Mg^{2+}, for example) for tertiary folding. Thus, the effect of macromolecular crowding on tertiary structures of RNA may be complicated. Using small angle X-ray scattering measurements it has been shown that, in the presence of polyethylene glycol (PEG), the 195 nucleotide *Azoarcus* ribozyme is more compact relative to $\phi = 0$ (Kilburn et al, 2010). It was concluded that excluded volume effects play a dominant role in the compaction of RNA in low molecular weight PEG. Interestingly, the transition to the folded state occurs at a lower Mg^{2+} concentration in the presence of PEG (Kilburn et al, 2010). Even if excluded volume interactions largely determine the stability of the folded states of RNA, a number of variables besides ϕ, such as size and shape of crowding agents, also contribute to the stability of RNA in the presence of inert crowding agents. Thus, a systematic study of the influence of macromolecular crowding on RNA is required.

It is known that, in contrast to proteins (Guo et al, 1992), the stability gap separating the native state and low energy excitations in RNA is small (Thirumalai and Hyeon, 2005), which implies that external factors (crowding or force) can modulate the stabilities and functions of RNA. For example, riboswitches undergo a transition

between two distinct conformations that have a profound influence on their functions (Montange and Batey, 2008). In this review article, we outline essential aspects of crowder-RNA interactions, with the particular emphasis on how crowding in the cellular environment may alter conformational equilibria related to enzymatic function. As a biologically relevant example, we discuss crowding effects on the transition between the hairpin (HP) and pseudoknot (PK) conformations (Figure 1) in the pseudoknot domain of human telomerase RNA, hTR (Theimer et al, 2003). The pseudoknot domain is conserved in different organisms and its activity is closely linked to chromosome stability (Blasco, 2003; Chen and Greider, 2004). However, the precise role of the PK and HP conformations of the pseudoknot domain in the context of telomerase activity is not known. Mutations that either increase or decrease the stability of the PK conformation result in a reduction in telomerase activity (Comolli et al, 2002; Theimer et al, 2005). Therefore, it is important to compare the impact of physical factors, such as macromolecular crowding, with that of naturally occurring chemical mutations. Our discussion of crowding presented in this review is original in two ways. First, we consider the effects of crowding on the conformational equilibrium between two folded states. Traditionally, discussions of crowding effects on biomolecules, mostly proteins, concern with the stability of the folded (active) state with respect to the unfolded (inactive) state. In addition, we establish a quantitative and novel connection between the magnitude of the crowding effect and activity of wild-type and mutant enzymes.

2 Computational models of RNA and crowders

Entropic stabilization, the mechanism by which macromolecular crowding stabilizes folded states of proteins and RNA in the excluded volume limit, is similar to spatial confinement, in a sense that crowders confine the biomolecule of interest to the interstitial space. Although analytical results exist for polymers confined to cavities with simple geometries, it is difficult to obtain accurate estimates for non-trivial confinement geometry associated with macromolecular crowding. Furthermore, unfolded RNA is a highly nonideal polymer whose conformational ensemble will be determined, among other things, by stacking propensities between adjacent bases and by the ionic strength of the buffer. Estimating how the conformational space of such a polymer will be reduced even in a simple geometrical confinement is a challenging task.

On the other hand, simulations have proven to be a useful tool in assessing the magnitude of entropic stabilization in response to varying external conditions. Coarse-grained models have been particularly effective in the studies of RNA folding, since they do not suffer from computational complexity associated with all-atom force fields (Lin and Thirumalai, 2008; Whitford et al, 2009; Cho et al, 2009; Feng et al, 2011; Denesyuk and Thirumalai, 2011). As a specific example of this class of techniques, we will be discussing results obtained with a widely appreciated coarse-grained representation of RNA, where each nucleotide is modeled by three interactions sites (TIS) — a phosphate, a sugar and a base (Hyeon and Thirumalai, 2005; Cho et al, 2009; Denesyuk and Thirumalai, 2011). We developed a force field in conjunction with the TIS model, which originally included stacking and hydrogen bond interactions as essential components in the

stability of RNA structures and was thermodynamically accurate in the limit of high ionic strength (Denesyuk and Thirumalai, 2011). The quantitative agreement of thermodynamic predictions of this force field with experiments is illustrated in Figure 3a. Subsequently, we added an electrostatic component to the TIS model to describe the RNA thermodynamics at different ionic concentrations (Denesyuk and Thirumalai, to appear elsewhere). The description of electrostatic effects in the model is based on Manning's concept of counterion condensation, which posits that counterions condense onto the RNA molecule and reduce the charge of phosphate groups from $-e$ to $-Qe$, where $Q < 1$ and e is the proton charge. The uncondensed mobile ions are treated using the Debye-Hückel theory. Therefore, the electrostatic energy of RNA in simulation is computed using

$$U_{\mathrm{EL}} = \frac{Q^2 e^2}{2\varepsilon} \sum_{i,j} \frac{\exp\left(-|\mathbf{r}_i - \mathbf{r}_j|/\lambda\right)}{|\mathbf{r}_i - \mathbf{r}_j|}, \tag{1}$$

where $|\mathbf{r}_i - \mathbf{r}_j|$ is the distance between two phosphates i and j, ε is the dielectric constant of water and λ is the Debye-Hückel screening length. We showed that, if the reduced phosphate charge Q was taken to be

$$Q = \frac{b}{l_{\mathrm{B}}}, \tag{2}$$

where l_{B} is the Bjerrum length and $b = 4.4$ Å, the measured thermodynamics of a variety of RNA sequences could be reproduced well over a wide range of temperatures and monovalent salt concentrations (Denesyuk and Thirumalai, to be published).

A generalized Lennard-Jones potential, introduced by Denesyuk and Thirumalai (2011), has been successfully employed to model interactions of RNA with the

spherical crowders of arbitrary size,

$$U_{\mathrm{LJ}}(r) = \varepsilon \frac{2R_i}{D_0}\left[\left(\frac{D_0}{r + D_0 - D}\right)^{12} - 2\left(\frac{D_0}{r + D_0 - D}\right)^{6} + 1\right],\ r \le D,$$
$$U_{\mathrm{LJ}}(r) = 0,\ r > D, \tag{3}$$

where r is the distance between the centers of mass of two interacting particles, D_0 is the effective penetration depth of the interaction, R_i is the radius of an RNA coarse-grained bead, r_{C} is the radius of a crowder, and $D = R_i + r_{\mathrm{C}}$. The ratio $2R_i/D_0$ in Eq. (3) is used to scale the interaction strength ε in proportion to the surface contact area. This potential correctly accounts for nonspecific surface interactions between spherical crowders representing large macromolecules and individual segments of the coarse-grained RNA.

Assessing the magnitude of crowding effect from simulations requires an accurate technique for calculating the folding free energies. To this end, a thermodynamic method has been proposed (Denesyuk and Thirumalai, to appear elsewhere), which does not require a structural order parameter to define folded and unfolded ensembles. To summarize, we perform a series of simulations at different temperatures in the range from T_1 to T_2, where T_1 and T_2 are on the order of the lowest and highest temperatures used in thermodynamic simulations or measurements. Using statistical mechanics techniques, we compute from these simulations the free energy of the molecule, G, as a function of temperature, T (Figure 2). If the population of the unfolded state is negligible at T_1, the free energy of the folded state at T_1, $G_{\mathrm{f}}(T_1)$, equals the computed free energy $G(T_1)$. Similarly, $G_{\mathrm{u}}(T_2) = G(T_2)$, if the population of the folded ensemble is statistically insignificant at the highest temperature T_2. Assuming similar equalities for the enthalpies and heat capacities of the folded and unfolded state, we can use thermodynamic

relationships between the free energies, enthalpies and heat capacities to extrapolate $G_{\rm f}(T_1)$ and $G_{\rm u}(T_2)$ to intermediate temperatures, at which both folded and unfolded states are populated (asymptotic lines in Figure 2). For any T between T_1 and T_2, geometric definition of the stability of the folded state with respect to the unfolded state, ΔG, is given in Figure 2.

3 Crowding effect is negligible for large crowders

The high density of macromolecules in the cell (volume fractions $\phi \approx 0.2 - 0.4$) reduces the space available for conformational fluctuations. Therefore, macromolecular crowding should result in a shift in the thermodynamic equilibrium between the HP and PK states of the hTR pseudoknot domain towards the more compact PK. To assess the extent to which PK is favored at $\phi \neq 0$, we discuss the simulation results (Denesyuk and Thirumalai, 2011) for the HP and PK states of the modified pseudoknot domain, ΔU177 (Figure 1). The molecular construct ΔU177 has been examined experimentally *in vitro* at $\phi = 0$ (Theimer et al, 2005), and the atomistic structures of its HP and PK conformations are available from the Protein Data Bank, codes 1NA2 and 2K96, respectively. Under native conditions, the RNA sequence in Figure 1 will predominantly populate the PK conformation. To obtain adequate statistics on both conformations, two independent sets of simulations were carried out, each modeling a limited subset of hydrogen bonds (Denesyuk and Thirumalai, 2011). In the first set of simulations, the RNA sequence could form only those hydrogen bonds that are found in the NMR structure of the PK. Similarly, in another set of simulations, only hydrogen bonds from the NMR structure of the HP were included. In the HP simulations strand

C166–A184 remained unbound in the folded state, because no hydrogen bonds could form between this strand and the remainder of the molecule. In this way, the interconversion between the PK and HP was eliminated and the HP structure could be sampled exhaustively. The stabilities of the PK and HP structures, $\Delta G_{\rm PK} = G_{\rm PK,f} - G_{\rm PK,u}$ and $\Delta G_{\rm HP} = G_{\rm HP,f} - G_{\rm HP,u}$, were obtained from the simulations using the technique illustrated in Figure 2. Since the unfolded state is effectively defined as a high-temperature state (in which all hydrogen bonds are broken) and the RNA sequence is the same in the PK and HP simulations, it was assumed that $G_{\rm PK,u} = G_{\rm HP,u}$. Therefore, the stability of the PK with respect to HP, $G_{\rm PK,f} - G_{\rm HP,f}$, was computed as $\Delta G_{\rm PK} - \Delta G_{\rm HP}$, without the need for explicit simulations of the PK-HP interconversion.

In order to illustrate the essential aspects of crowding effects on RNA, we consider spherical particles with radius $r_{\rm C}$. For monodisperse particles, the volume fraction is $\phi = 4\pi r_{\rm C}^3 \rho/3$, where ρ is the number density. Thus, ϕ can be changed by increasing or decreasing ρ or by altering the size of the crowding particles. In this review, we fix $\phi = 0.3$ and examine the consequences of changing $r_{\rm C}$. Based on general theoretical considerations (Asakura and Oosawa, 1958; Shaw and Thirumalai, 1991) it can be shown that, in the colloid limit $r_{\rm C} > R_{\rm G}^0$, the crowding agents would have negligible effects on RNA stability. Here, $R_{\rm G}^0$ is the size of RNA in the absence of the crowding agent. It is only in the opposite polymer limit, $r_{\rm C} < R_{\rm G}^0$, that the crowding particles would affect RNA stability. We therefore expect that the magnitude of the crowding effect should depend on the ratio $r_{\rm C}/R_{\rm G}^0$.

In Figure 3a we show the HP melting profile, taken to be the negative derivate of the number of intact base pairs $N_{\rm BP}$ with respect to $k_{\rm B}T$, for the crowder radius

$r_C = 26$ Å (Denesyuk and Thirumalai, 2011). Such crowders are larger than the radius of gyration of strand G93–C121 in the unfolded state, $R_G^0 = 20$ Å (Figure 1c). As discussed above, large crowders have minimal effects on the melting of the HP even at $\phi = 0.3$. For a fixed ϕ, the average distance between two spherical crowders will increase with the crowder size. If the unfolded hairpin can easily fit in the interstitial space, the folding/unfolding transition will not be affected significantly by the presence of crowders. For $\phi = 0.3$ and the crowder radius $r_C = 26$ Å, which is only slightly larger than R_G^0, the increase ΔT in the melting temperature is 1.5 °C for stem 1 of the HP and is negligible for stem 2 (Figure 3a). Further increase in r_C results in $\Delta T \approx 0$ for both stems (data not shown).

Figure 3a also shows the melting profile of the HP in a ternary mixture of crowders, containing volume fractions $\phi = 0.11$, 0.11 and 0.08 of particles with $r_C = 104$ Å, 52 Å and 26 Å, respectively (Denesyuk and Thirumalai, 2011). The sizes and volume fractions of individual components in the model mixture correspond to the ribosome, large enzymatic complexes and relatively small individual proteins, found in *E. coli*. Because all the values of r_C in the *E. coli* mixture are larger than R_G^0, we expect only small changes in the melting profile of the HP (Figure 3a). For the total volume fraction of 0.3, the melting temperature of the HP stem 1 increases only by 2 °C with respect to $\phi = 0$ (Figure 3a). Interestingly, the effect of the *E. coli* mixture is similar in magnitude to that of a monodisperse suspension with $r_C = 26$ Å and $\phi = 0.3$. In contrast, a monodisperse suspension with $r_C = 26$ Å and $\phi = 0.08$, which is equivalent to the smallest particle component in the mixture, has negligible effect on the melting of the HP (Figure 3a).

To summarize, the crowding effect of polydisperse mixtures is largely the effect of the smallest particle component, but taken at the total volume fraction of the

mixture. As we discuss in the next section, the excess stability of the folded state due to crowding decreases nonlinearly with the radius of the crowding particle r_C. We therefore propose that, for crowding in the cellular environment, the main role of large macromolecules will be to increase the effective volume fraction of the relatively small macromolecules.

4 Role of crowder size in the PK-HP equilibrium

The sensitivity of the crowding effect to the relative sizes of RNA and crowders is at the basis of the equilibrium shift in the hTR pseudoknot domain. Figure 3b shows the change in stability of the HP and PK at 37 °C induced by monodisperse crowders for different crowder radii r_C ($\phi = 0.3$). As anticipated by arguments given above, the magnitude of the excess stability $\Delta G(0.3) - \Delta G(0)$ is small if $r_C/R_G^0 > 1$ and increases sharply for $r_C/R_G^0 < 1$. Note that the crowding effect is larger for the PK for all values of r_C (Figure 3b), indicating an equilibrium shift towards this conformation. The discussed change in the PK-HP relative stability is of entropic origin. The unfolded ensembles of the PK and HP are equivalent, as discussed above, and will therefore be depleted by macromolecular crowding to a similar degree. The compact folded PK is, to a first approximation, unaffected by crowding. However, the folded HP contains an unbound strand C166–A184 (Figure 1), whose loose conformations will be restricted in a crowded environment. Therefore, the excess stability of the PK with respect to HP is due to a partial suppression of the HP folded ensemble by macromolecular crowding.

The crowder radius $r_C = 12$ Å corresponds to the size of an average protein *in vivo*. For $\phi = 0.3$ and $r_C = 12$ Å, we have $\Delta G_{PK}(0.3) - \Delta G_{PK}(0) = -2.4$

kcal/mol and $\Delta G_{\rm HP}(0.3) - \Delta G_{\rm HP}(0) = -1.0$ kcal/mol, which amounts to the relative stabilization of the PK conformation by -1.4 kcal/mol (Figure 3b). Below we analyze this value in the context of standard changes in the PK stability caused by mutations.

5 Implications for function

As mentioned in the Introduction, changes in the relative stability of the HP and PK conformations of the hTR pseudoknot domain compromise the enzyme activity. The estimate of the crowding effect in a typical cellular environment, $\Delta\Delta G = -1.4$ kcal/mol, allows us to assess the extent to which macromolecules could regulate telomerase activity. Experimental data on hTR mutants (Comolli et al, 2002; Theimer et al, 2005) clearly demonstrate that enzyme activity decreases when plotted as a function of $|\Delta\Delta G^*| = |\Delta G^*_{\rm PK}(0) - \Delta G_{\rm PK}(0)|$, where $\Delta G^*_{\rm PK}(0)$ and $\Delta G_{\rm PK}(0)$ are the stabilities of mutant and wild-type pseudoknots at $\phi = 0$ (Figure 4). The majority of mutations destabilize the PK, $\Delta\Delta G^* > 0$ (black squares in Figure 4) and only two mutants have $\Delta\Delta G^* < 0$ (red stars in Figure 4). For destabilizing mutants the reduction in activity, α, was shown by Denesyuk and Thirumalai (2011) to follow the exponential dependence, $\alpha = \exp(-0.6\Delta\Delta G^*)$ (thick curve in Figure 4). The naturally occurring destabilizing mutations DKC and C116U have been linked to diseases dyskeratosis congenita and aplastic anemia, respectively (Vulliamy et al, 2002; Fogarty et al, 2003). The DKC and the stabilizing ΔU177 mutations have been studied *in vivo* (green symbols in Figure 4), as well as *in vitro*. In both cases, mutant telomerase *in vivo* was found to be significantly

less active than the corresponding construct *in vitro*, suggesting that a number of factors determine the activity of telomerase *in vivo*.

Although macromolecular crowding enhances the stability of the PK state, the crowding effect ($\Delta\Delta G = -1.4$ kcal/mol) is less than the stability changes caused by mutations. In Figure 4 the grey area marks the domain of potential mutants with $\Delta\Delta G^* > 0$, whose activity may be completely restored by macromolecular crowding. All experimentally studied mutants fall outside the marked domain, including the two disease related mutants DKC and C116U. Nevertheless, due to the strong dependence of enzyme activity on $\Delta\Delta G^*$, the effect of crowding on telomerase function may be significant. We estimate that the activity of telomerase can be up- or down-regulated by more than two-fold in response to density fluctuations in its immediate environment. Furthermore, due to the expected dynamical heterogeneities in cells, there will be variations in enzyme activity in different cell regions.

6 Crowding effects on RNA at different ionic strengths

Entropic stabilization mechanism (Cheung et al, 2005) implies that crowding increases the stability of the folded state by reducing the population of expanded conformations in the unfolded state. Therefore, we expect that the magnitude of the crowding effect will be sensitive to the ionic strength of the RNA buffer, since the latter determines the size of the unfolded RNA. The quantitative discussion above assumed the limit of high ionic strength. As the buffer ionic concentration c is lowered, the screening of the negative charge on the RNA sugar-phosphate backbone becomes less efficient, which in turn increases the mean radius of gyra-

tion of conformations in the unfolded state. The function $R_G(c)$ for the unfolded PK is shown in Figure 5a in the absence (black diamonds) and presence (green circles) of crowding. The same general trend is observed in both cases, with the R_G values being consistently smaller when crowders are present for the entire range of c. In accord with our predictions, the crowder-induced stabilization of the folded PK becomes more significant at low ionic strengths (red squares in Figure 5a). Interestingly, the stabilization effect increases rapidly upon lowering c from 1 M to 0.1 M, but shows little change when c is lowered further to below 0.1 M. The underlying reason for such behavior can be traced to the probability distributions $p(R_G)$ in the unfolded state (Figure 5b). For a given crowder solution, we can identify a typical size of the cavity which will be free of any crowders. If the radius of gyration of RNA conformations is such that they fit into the cavity, these conformations will not be perturbed by crowding. On the other hand, the population of conformations with R_G larger than the typical cavity size will be significantly depleted by crowding. For $\phi = 0.3$ and $r_C = 12$ Å, we can infer the size of a standard empty cavity from the distributions $p(R_G)$ at high ionic strength ($c = 1$ M, Figure 5b). Note that $p(R_G)$ decreases for $R_G > 20$ Å when crowders are present (green solid line in Figure 5b), but $p(R_G)$ increases with R_G around 20 Å in the absence of crowders (black solid line in Figure 5b). This indicates that the crowders significantly perturb the unfolded conformations with R_G larger than 20 Å, which can serve as an upper estimate of the smallest RNA size affected by crowders. When c decreases, the distribution $p(R_G)$ shifts to larger R_G, increasing the fraction of the unfolded conformations affected by crowders. At $c = 0.1$ M, all statistically significant values of R_G in the unfolded state fall within the range $R_G > 20$ Å, both for $\phi = 0$ (black diamonds in Figure 5b) and for $\phi = 0.3$ (green circles in

Figure 5b), so that the entire distribution $p(R_G)$ is depleted due to crowding. This explains why the crowding-induced stabilization is almost constant below 0.1 M, even if the average R_G continues to increase rapidly all the way to 0.01 M (symbols in Figure 5a).

7 RNA becomes compact as ϕ increases

The reduction in conformational space accessible to RNA should increase with ϕ, for a fixed r_C. Thus, we expect that R_G should decrease as ϕ increases. This is precisely what is observed in experiments (Kilburn et al, 2010), which show that at all concentrations of Mg^{2+} the *Azoarcus* ribozyme becomes more compact as the volume fraction of the crowding agent (PEG) increases (Figure 6). Interestingly, the midpoint of the folding transition c_m — the concentration of Mg^{2+} at which the folded and unfolded states of the *Azoarcus* ribozyme have equal populations — also decreases as ϕ increases (Figure 6). This finding can be readily explained in terms of the entropic stabilization mechanism (Cheung et al, 2005) and suggests that, to a first approximation, PEG behaves as an inert hard sphere crowding agent. Based on our considerations from the previous section, we predict that the shift in c_m due to crowding will also depend on the concentration of monovalent counterions in the RNA buffer, a prediction that is amenable to experimental test. In addition, it would be of interest to perform experiments at a fixed ϕ but varying r_C, which can be changed by decreasing or increasing the molecular weight of PEG.

8 Conclusions

The phenomena discussed here illustrate just one aspect of crowding effects on RNA. There are other physical and chemical factors that could determine how crowding modulates RNA stability, and hence its function. The interplay between electrostatic interactions, hydration of phosphate groups and crowding particles, as well as the shape of crowding particles, could potentially present a much more nuanced picture than the simplest case considered here. Even though these effects are important and warrant further study, the analysis presented here is important in establishing the maximum increase in stability that can be realized when excluded volume interactions dominate. From this perspective, our conclusion that the crowding effects cannot fully restore telomerase activity *in vivo* is robust. In future work, it will be important to connect the consequences of crowding effects on RNA folding with the RNA activity under cellular conditions.

Acknowledgements We are grateful to Sarah Woodson for providing Figure 6. Our work was supported by a grant from the National Science Foundation (CHE 09-10433).

Conflict of Interest: None

References

Asakura S, Oosawa F (1958) Interaction between particles suspended in solutions of macromolecules. J Polym Sci 33(126):183–192

Blasco M (2003) Telomeres and cancer: a tale with many endings. Curr Opin Genet Dev USA 13(1):70–76

Chen J, Greider C (2004) An emerging consensus for telomerase RNA structure. Proc Natl Acad Sci USA 101(41):14,683–14,684

Cheung M, Klimov D, Thirumalai D (2005) Molecular crowding enhances native state stability and refolding rates of globular proteins. Proc Natl Acad Sci USA 102(13):4753–4758

Cho SS, Pincus DL, Thirumalai D (2009) Assembly mechanisms of RNA pseudoknots are determined by the stabilities of constituent secondary structures. Proc Natl Acad Sci USA 106(41):17,349–17,354

Comolli L, Smirnov I, Xu L, Blackburn E, James T (2002) A molecular switch underlies a human telomerase disease. Proc Natl Acad Sci USA 99(26):16,998–17,003

Denesyuk NA, Thirumalai D (2011) Crowding promotes the switch from hairpin to pseudoknot conformation in human telomerase RNA. J Am Chem Soc 133(31):11,858–11,861

Dhar A, Samiotakis A, Ebbinghaus S, Nienhaus L, Homouz D, Gruebele M, Cheung MS (2010) Structure, function, and folding of phosphoglycerate kinase are strongly perturbed by macromolecular crowding. Proc Natl Acad Sci USA 107(41):17,586–17,591

Elcock AH (2010) Models of macromolecular crowding effects and the need for quantitative comparisons with experiment. Curr Opin Struct Biol 20(2):196–206

Feng J, Walter NG, Brooks CL III (2011) Cooperative and directional folding of the preq(1) riboswitch aptamer domain. J Am Chem Soc 133(12):4196–4199

Fogarty P, Yamaguchi H, Wiestner A, Baerlocher G, Sloand E, Zeng W, Read E, Lansdorp P, Young N (2003) Late presentation of dyskeratosis congenita

as apparently acquired aplastic anaemia due to mutations in telomerase RNA. Lancet 362(9396):1628–1630

Guo Z, Thirumalai D, Honeycutt J (1992) Folding kinetics of proteins — a model study. J Chem Phys 97(1):525–535

Hall D, Minton AP (2003) Macromolecular crowding: qualitative and semiquantitative successes, quantitative challenges. BBA-Proteins Proteom 1649(2):127–139

Homouz D, Perham M, Samiotakis A, Cheung MS, Wittung-Stafshede P (2008) Crowded, cell-like environment induces shape changes in aspherical protein. Proc Natl Acad Sci USA 105(33):11,754–11,759

Hyeon C, Thirumalai D (2005) Mechanical unfolding of RNA hairpins. Proc Natl Acad Sci USA 102(19):6789–6794

Kilburn D, Roh JH, Guo L, Briber R, Woodson SA (2010) Molecular crowding stabilizes folded RNA structure by the excluded volume effect. J Am Chem Soc 132(25):8690–8696

Lin JC, Thirumalai D (2008) Relative stability of helices determines the folding landscape of adenine riboswitch aptamers. J Am Chem Soc 130(43):14,080–14,081

Minton A (2001) The influence of macromolecular crowding and macromolecular confinement on biochemical reactions in physiological media. J Biol Chem 276(14):10,577–10,580

Minton AP (1981) Excluded volume as a determinant of macromolecular structure and reactivity. Biopolymers 20(10):2093–2120

Minton AP (2005) Models for excluded volume interaction between an unfolded protein and rigid macromolecular cosolutes: Macromolecular crowding and pro-

tein stability revisited. Biophys J 88(2):971–985

Montange RK, Batey RT (2008) Riboswitches: Emerging themes in RNA structure and function. Ann Rev Biophys 37:117–133

Pincus D, Hyeon C, Thirumalai D (2008) Effects of trimethylamine n-oxide (tmao) and crowding agents on the stability of RNA hairpins. J Am Chem Soc 130(23):7364–7372

Shaw M, Thirumalai D (1991) Free polymer in a colloidal solution. Phys Rev A 44(8):R4797–R4800

Theimer C, Finger L, Trantirek L, Feigon J (2003) Mutations linked to dyskeratosis congenita cause changes in the structural equilibrium in telomerase RNA. Proc Natl Acad Sci USA 100(2):449–454

Theimer C, Blois C, Feigon J (2005) Structure of the human telomerase RNA pseudoknot reveals conserved tertiary interactions essential for function. Mol Cell 17(5):671–682

Thirumalai D, Hyeon C (2005) RNA and protein folding: Common themes and variations. Biochemistry 44(13):4957–4970

Vulliamy T, Marrone A, Dokal I, Mason P (2002) Association between aplastic anaemia and mutations in telomerase RNA. Lancet 359(9324):2168–2170

Whitford PC, Schug A, Saunders J, Hennelly SP, Onuchic JN, Sanbonmatsu KY (2009) Nonlocal helix formation is key to understanding s-adenosylmethionine-1 riboswitch function. Biophys J 96(2):L7–L9

Zhou HX, Rivas G, Minton AP (2008) Macromolecular crowding and confinement: Biochemical, biophysical, and potential physiological consequences. Ann Rev Biophys 37:375–397

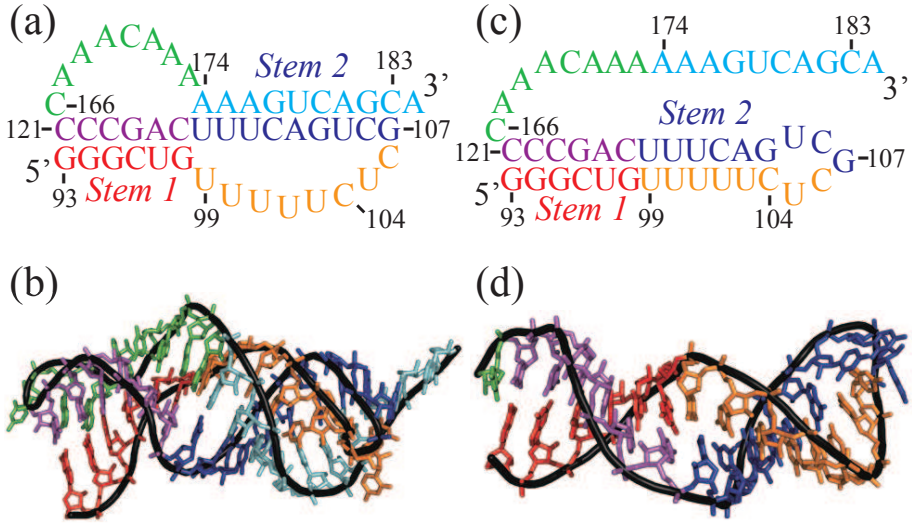

Fig. 1 Graphic adopted from Denesyuk and Thirumalai (2011). Secondary and tertiary structures of the pseudoknot (PK) and hairpin (HP) conformations for ΔU177. The sequence of ΔU177 was chosen to match experiments, in which nucleotides 122–165 and 177 were deleted to facilitate structural studies (Theimer et al, 2005). (a) PK secondary structure. (b) PK tertiary structure. (c) HP secondary structure. (d) HP tertiary structure. NMR structure of the HP includes residues G93 to C166 only (PDB code 1NA2). To quantify the effect of crowders on the PK-HP equilibrium, we added an unstructured tail A167–A184 to the NMR structure (panel c). This inclusion ensures that identical RNA sequences are used in simulations of the PK and HP conformations.

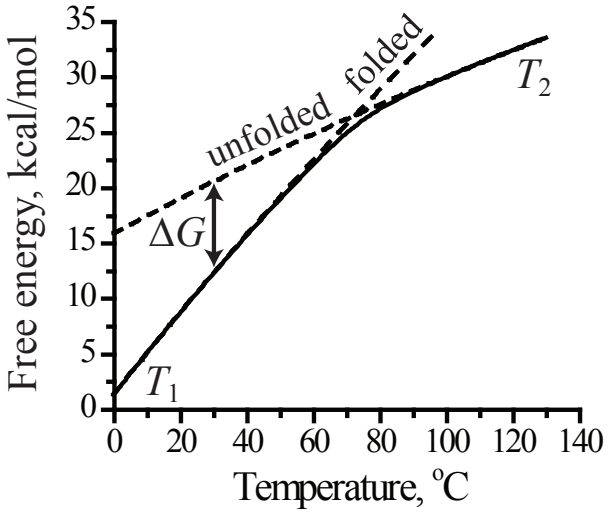

Fig. 2 Geometrical definition of the stability ΔG of the folded state. The solid curve illustrates the total free energy of a system as a function of temperature, computed in simulation. The free energies of individual folded and unfolded ensembles (dashed curves) are obtained as described in the text.

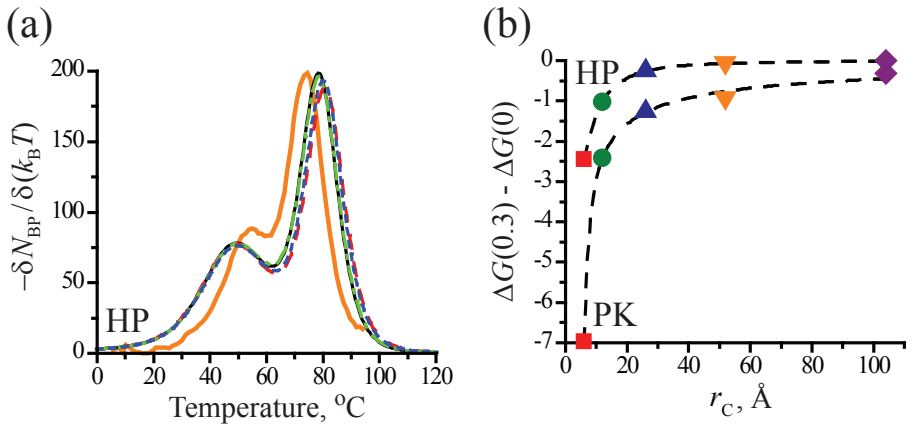

Fig. 3 (a) Melting profiles of the HP in various crowding environments at 1 M or higher monovalent salt concentration. Black solid curve: without crowders. Red dashed curve (the model *E. coli* mixture): $\phi = 0.11$ of crowders with $r_C = 104$ Å, $\phi = 0.11$ of crowders with $r_C = 52$ Å and $\phi = 0.08$ of crowders with $r_C = 26$ Å. Green dashed-dotted curve: $\phi = 0.08$ of crowders with $r_C = 26$ Å. Blue dotted curve: $\phi = 0.3$ of crowders with $r_C = 26$ Å. The thick orange curve is the experimental UV data at 200 mM KCl from Figure 2b in Theimer et al (2003), divided by 5.53×10^{-5}. The two peaks indicate melting of stems 1 and 2 of the HP (Figure 1c). The peak positions (melting temperatures) and the overall width of the melting curve (melting range) serve as a measure of agreement between theory and spectroscopic data. (b) Changes in stability (kcal/mol) of the HP and PK at 37 °C due to crowders at $\phi = 0.3$, as a function of the crowder radius r_C.

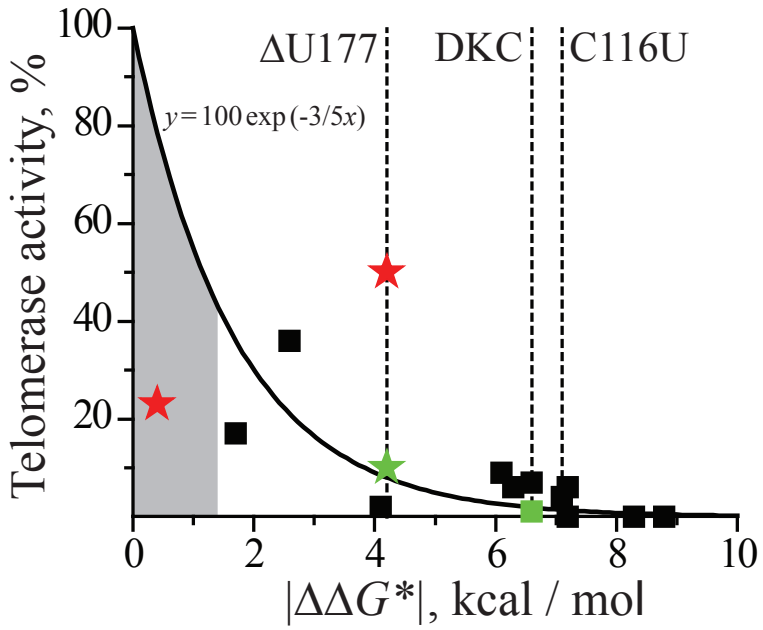

Fig. 4 Graphic adopted from Denesyuk and Thirumalai (2011). Activity of mutant telomerase normalized to wild-type activity (100%), as a function of the magnitude of the stability difference between mutant and wild-type pseudoknots. Three mutants, ΔU177, DKC and C116U, are explicitly marked. The *in vitro* data for destabilizing (black squares) and stabilizing (red stars) mutations are from Table 2 in Theimer et al (2005). Green symbols show the *in vivo* data for ΔU177 and DKC from Comolli et al (2002). The experimental data for destabilizing mutations is fit to the exponential function (solid curve). Grey area marks the range of stability differences that can be accommodated by crowding.

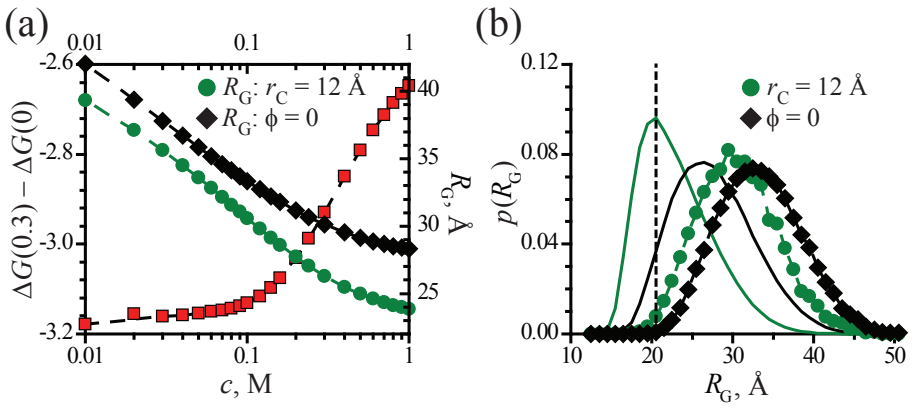

Fig. 5 (a) The radius of gyration of the unfolded PK (right axis), as a function of the monovalent ion concentration c, for $\phi = 0$ (black diamonds) and $\phi = 0.3$, $r_C = 12$ Å (green circles). Red squares show the excess stability of the PK due to crowding, $\Delta G_{PK}(0.3) - \Delta G_{PK}(0)$, for $r_C = 12$ Å (left axis). (b) Probability distributions $p(R_G)$ of the radius of gyration of the unfolded PK for $\phi = 0$ and $c = 1$ M (black solid line), for $\phi = 0$ and $c = 0.1$ M (black diamonds), for $\phi = 0.3$, $r_C = 12$ Å and $c = 1$ M (green solid line), and for $\phi = 0.3$, $r_C = 12$ Å and $c = 0.1$ M (green circles). The vertical dashed line indicates the smallest size of RNA conformations that will be perturbed by crowders with $\phi = 0.3$ and $r_C = 12$ Å.

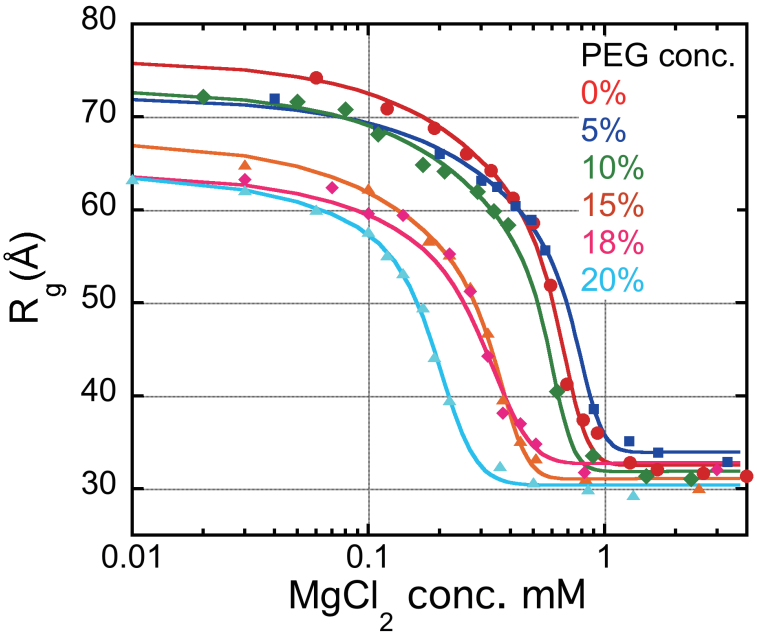

Fig. 6 Graphic adopted from Kilburn et al (2010). Small angle X-ray scattering measurements of the radius of gyration of the *Azoarcus* ribozyme for different concentrations of Mg^{2+} ions and PEG.